Earthquakes and Structures, *Vol. 18, No. 2* (*2020*) *215-222*
DOI: https://doi.org/10.12989/eas.2020.18.2.215

The effect of cyclic loading on the rubber bearing with slit damper devices based on finite element method

Mahdi Saadatnia[1a], Hossein Tajmir Riahi*[1,2] and Mohsen Izadinia[1b]

[1]*Department of Civil Engineering, Najafabad Branch, Islamic Azad University, Najafabad, Iran*
[2]*Department of Civil Engineering, University of Isfahan, Isfahan, Iran*

(*Received January 2, 2020, Revised January 20, 2020, Accepted January 23, 2020*)

Abstract. In this paper, slit steel rubber bearing is presented as an innovative seismic isolator device. In this type of isolator, slit steel damper is an energy dissipation device. Its advantages in comparison with that of the lead rubber bearing are its simplicity in manufacturing process and replacement of its yielding parts. Also, slit steel rubber bearing has the same ability to dissipate energy with smaller value of displacement. Using finite element method in ABAQUS software, a parametric study is done on the performance of this bearing. Three different kinds of isolator with three different values of strut width, 9, 12 and 15 mm, three values of thickness, 4, 6 and 8 mm and two steel types with different yield stress are assessed. Effects of these parameters on the performance characteristics of slit steel rubber bearing are studied. It is shown that by decreasing the thickness and strut width and by selecting the material with lower yield stress, values of effective stiffness, energy dissipation capacity and lateral force in the isolator reduce but equivalent viscous damping is not affected significantly. Thus, by choosing appropriate values for thickness, strut width and slit steel damper yield stress, an isolator with the desired behavior can be achieved. Finally, the performance of an 8-storey frame with the proposed isolator is compared with the same frame equipped with LRB. Results show that SSRB is successful in base shear reduction of structure in a different way from LRB.

Keywords: slit steel rubber bearing; base-isolation; cyclic behavior; energy dissipation; lead rubber bearing

1. Introduction

The fundamental natural period transition of a structure into an elongated period is the concept of seismic base-isolation to mitigate damage in civil structures. The superstructure behavior in base-isolated structure is mostly linear. A complete literature review of this issue is run by Warn and Ryan (2012). Rubber bearings are the most popular devices used for this purpose and various types of rubber bearing are studied including natural rubber bearing (NRB) (Iizuka 2000, Sanchez *et al.* 2012), high damping rubber bearing (HDRB) (Bhuiyan *et al.* 2009) and lead rubber bearing (LRB) (Ghobarah and Ali 1990, Ryan *et al.* 2005). The LRB is the most famous bearing shaped as a rectangular or circular laminated pad to be fixed at the top and bottom ends of the supporting steel plates. In addition to its flexibility, a base isolation device must be able to dissipate energy in order to prevent large displacements. The lead core of LRB is an energy dissipater which generates the necessary damping. HDRB consists of additional materials to enhance the necessary damping (Tiong *et al.* 2014). After a destructive earthquake, the reshaped lead of LRB will be subjected to a drop in yield stress and its effective stiffness and dissipated energy capacity decrease (Paul 2016, Choi *et al.* 2005, Kalpakidis and Constantinou 2008) and in this situation, it is reasonable to replace the entire isolator. In LRB the lead core is located in the interconnected layers of rubber and steel, indicating its non-replacement. Due to high rubber deformation and cyclic behavior of HDRBs in strong earthquakes the rubber is damaged, thus, a complete change in the bearing behavior is happened (Yoon *et al.* 2013, Zhou *et al.* 2018, Kim *et al.* 2014). There are many studies regarding other energy-dissipating devices and their applications in seismic isolation devices. A U-shaped damper in rubber bearings is adopted by Oh *et al.* (2013) to stabilize the hysteretic response. The shape memory alloy (SMA) wire as a damper in rubber bearing is introduced by Dezfuli and Alam (2013, 2015) which can restore the initial form after deformation. As to SMA-LRB isolated highway bridge, the effect of constitutive models on the seismic response is assessed by Dezfuli *et al.* (2017). They revealed that applying SMA increase the horizontal stiffness of bearing and reduce the shear strain demand of LRB which leads to highway bridge deck displacement. The SMA-LRB containing ferrous shape memory alloy wires is applied to resist seismicity in highway bridges (Hedayati Dezfuli and Alam 2017). They concluded that in comparison with LRB, applying SMA-LRB on bridges reduces shear strain demand by about 46% and increases energy dissipation capacity by about 31%.

Rubber Bearing incorporated with steel ring damper (NRB-SRD) is assessed by (Sheikhi and Fathi 2019). A better performance in energy dissipation compared to SMA-LRB and HDRB is observed in NRB-SRD. Ring Rubber Bearing is an innovative base isolator where lead is

*Corresponding author, Professor
E-mail: tajmir@eng.ui.ac.ir
[a]Ph.D. Student
[b]Professor

ISSN: 2092-7614 (Print), 2092-7622 (Online)

replaced by a rubber cylinder surrounded by steel rings (Talaeitaba *et al.* 2019). A new hybrid isolator consisting of elastomeric bearing, sliding parts and yielding dampers named friction–yielding– elastomeric bearing is proposed by (Haeri *et al.* 2019), with a more appropriate and stable performance at all shear strains in comparison to LRB.

Recently, a similar study by Saadatnia *et al.* (2019) assessed the application of perforated yielding shear plates as energy dissipating device instead of the lead core in LRB. They showed that although perforated yielding shear plate rubber bearing can bear lower shear strain, this isolator dissipates more energy at lower lateral displacement and therefore it can meet the characteristics of LRB at lower shear strain.

The steel slit damper (SSD) is another type of dampers that are mostly applied at the beam to column connections (Oh *et al.* 2009, Lee and Kim 2015). Lateral displacement of slit damper has shear yielding and flexural yielding mechanisms (Amadeo *et al.* 1998). It is reported that slit damper has adequate energy dissipative capacity as well as high stiffness and can be considered as an appropriate device instead of lead in LRB. Recently, there are many studies regarding steel slit dampers. Some authors focused on the new types of hybrid dampers which are composed of a friction damper and steel strip damper (Kim and Shin 2017, Lee *et al.* 2016, Lee *et al.* 2017). Bagheri *et al.* (2016) run a shaking table test and studied the seismic response characteristics of concentrically braced steel structure with and without hysteretic dampers. An hourglass-shaped strip damper (HSD) was used by Lee *et al.* (2016b) to improve the seismic response characteristics of the conventional slit damper. Kim and Jeong used a proper amount of steel plate slit dampers to keep the seismic response of low-rise asymmetric structures within a given target performance level (Kim and Jeong 2016).

In this study, lead core in LRB is replaced by steel slit dampers and seismic response characteristics of this new bearing are studied using ABAQUS software. The steel slit dampers are connected to the four sides of the bearing at the top and bottom steel plates of the bearing. This replacement has some advantages and some disadvantages which are investigated. First, LRB and SSD are modeled and studied numerically using finite element method (FEM). The cyclic behavior is assessed and results are compared with the experimental ones reported by others. Next, the lead core is replaced by SSDs to allow the assessment of the cyclic behavior of the force-displacement of the new bearing. Then, the effective stiffness, energy dissipation capacity and equivalent viscous damping of the bearing are obtained and compared with that of the corresponding LRB. Finally, the effects of SSD's thickness, mechanical properties and its strip width on the performance characteristics of slit steel rubber bearing (SSRB) are examined. Application of SSRB on an 8-storey frame is also investigated and its results are compared with the results of the same frame equipped with LRB.

2. Analytical behavior of SSD

Slit dampers can be applied on the top of inverted-V braces (Bagheri *et al.* 2016), in beam-to-column connections (Oh *et al.* 2009, Saffari *et al.* 2013) or in seesaw energy dissipation systems (Tagawa *et al.* 2016). The shape and dimensions of a steel slit damper are presented in Fig. 1. It is assumed that one side of the damper is fixed and the other on is roller supported. Slit dampers are considered to have both shear yielding and flexural yielding mechanisms. In these types of dampers, plastic deformation of the vertical strut causes energy dissipation. It is reported by previous studies that slit dampers have high energy dissipation capacity and high stiffness and can be used as appropriate dampers to control the relative displacement of structure floors. By considering flexural moment and shear force, the yield force and ultimate force of a slit damper can be calculated as (Oh *et al.* 2009)

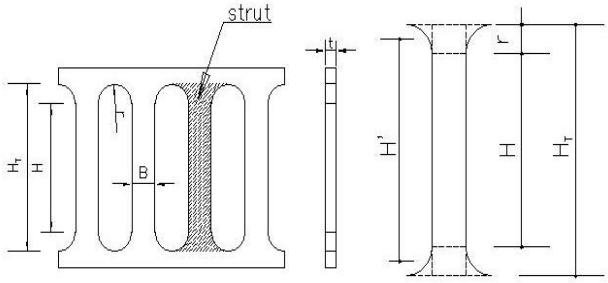

Fig. 1 Geometrical parameters of the slit damper

$$P_y = \min\left\{ n\frac{\sigma_y t B^2}{2H'}, n\frac{2\sigma_y t B}{3\sqrt{3}} \right\}, \quad (1)$$

$$P_u = \min\left\{ n\frac{\sigma_u t B^2}{2H'}, n\frac{2\sigma_u t B}{3\sqrt{3}} \right\}, \quad (2)$$

in which n, σ_y, σ_u, t, B and H' are number of struts, yield stress, ultimate stress, thickness and width of the strut and equivalent height of the slit damper, respectively (see Fig. 1). Also, the yield displacement of a slit damper (δ_y) can be expressed as (Amadeo *et al.* 1998)

$$\delta_y = \delta_b + \delta_s = \frac{P_y (H')^3}{nEtB^3}\left(1 + 3\ln\frac{H_T}{H'}\right) + \frac{3P_y H'}{2ntBG}\left(1 + \ln\frac{H_T}{H'}\right), \quad (3)$$

where δ_b and δ_s are the components of the displacement due to the flexural and shear deformations, respectively; and E, G and H_T are modulus of elasticity, shear modulus and the total height of the strut (see Fig. 1). It is shown by (Amadeo *et al.* 1998) that Eq. (3) can be simplified as

$$\delta_y = \frac{1.5P_y H_T}{nEtB}\left[\left(\frac{H'}{B}\right)^2 + 2.6\right] \quad (4)$$

3. Verification

3.1 SSD Verification

In order to validate the presented model, FEM results obtained using C3D8R solid elements in ABAQUS

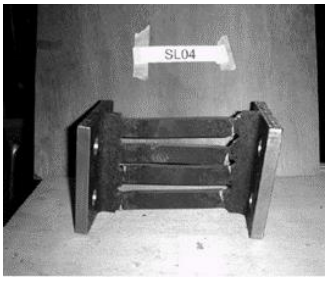

(a)

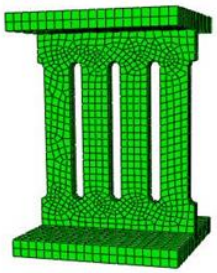

(b)

Fig. 2 (a) The SL04 specimen tested by Chan and Albermani (Chan and Albermani 2008) and (b) FEM model of SL04

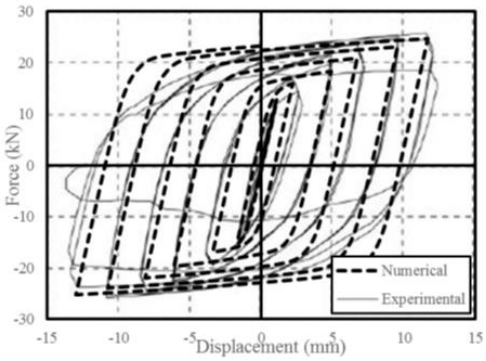

Fig. 3 Comparison of the presented numerical analysis with the experimental results (Chan and Albermani 2008) for hysteresis cycle of the SSD

Table 1 LRB size

Type of bearing	Lead rubber bearing
Cross-section (mm)	200×200
Shear modulus (MPa)	0.78
Number of layers rubber	7
Thickness of one layer rubber (mm)	5
Number of inner steel plates	6
Thickness of inner steel plates (mm)	2.3
Diameter of lead plug (mm)	40

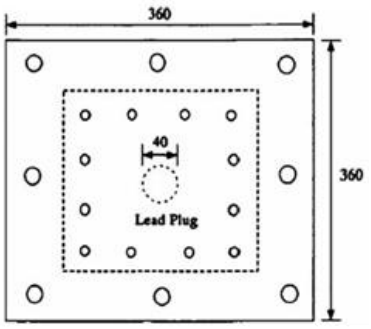

(a) Plane view (mm)

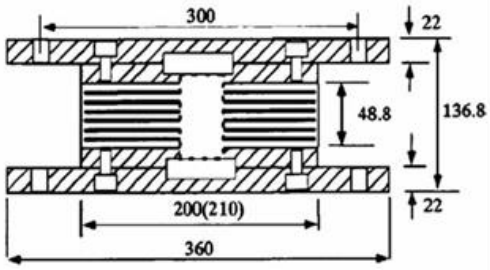

(b) Side view (mm)

Fig. 4 The LRB size (Abe *et al.* 2004)

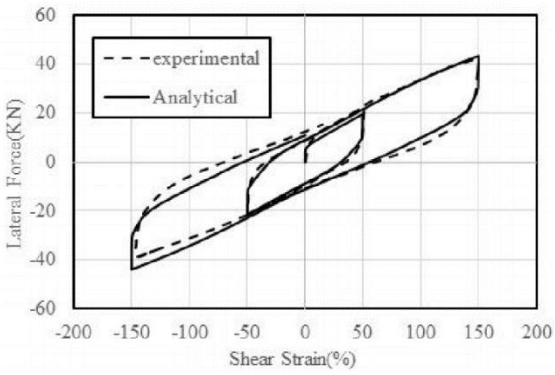

Fig. 5 Comparison of the presented numerical analysis with the experimental data (Abe *et al.* 2004) for hysteresis cycle of the LRB

software are compared with the experimental ones reported by (Chan and Albermani, 2008). They studied nine types of SSD and as depicted in Fig. 2, one of them which is called SL04 is used in this paper to validate the presented model. This specimen is cut from a single segment of a wide-flange section. Its depth, flange width, web thickness and flange thickness are 161.8 mm, 152.2 mm, 8 mm and 11.5 mm, respectively. FEM model is analyzed using elements of size 5 mm. The material properties are elastic-perfectly plastic with a 316.5 MPa yield stress in relation to Mises plasticity. An elasto-plastic behavior with combined hardening is of concern here, in order to perform numerical simulation in the cyclic field of the steel, by restraining the degrees of freedom at the lower surface of the SSD. The bottom surface of SSD remains constant and the upper surface moves subject to a specific loading protocol. A comparison is presented in Fig. 3 between hysteretic curves obtained using FEM and the experimental ones reported by (Chan and Albermani 2008). A comparison between presented results and the experimental ones confirms high accuracy of the presented numerical simulation.

3.2 Verification of LRB

In 2004, (Abe *et al.* 2004) presented some experimental results on samples of LRB which is illustrated in Fig. 4 and is described in Table 1. One-third of the real bearings installed at a highway bridge in Japan constitutes the model size. Using the hybrid C3D8H element for modeling the rubber, the bearing is modeled in ABAQUS software. The rubber is modeled based on the Neo hook model (Asl *et al.* 2014) and its viscous damping ratios is considered to be about 2-3%.

The lead is considered to have a bilinear isotropic hardening behavior modeled with the modulus of elasticity of 16 MPa and yield stress of 10 MPa. Steel plates are modeled using C3D8R element and are assumed to be

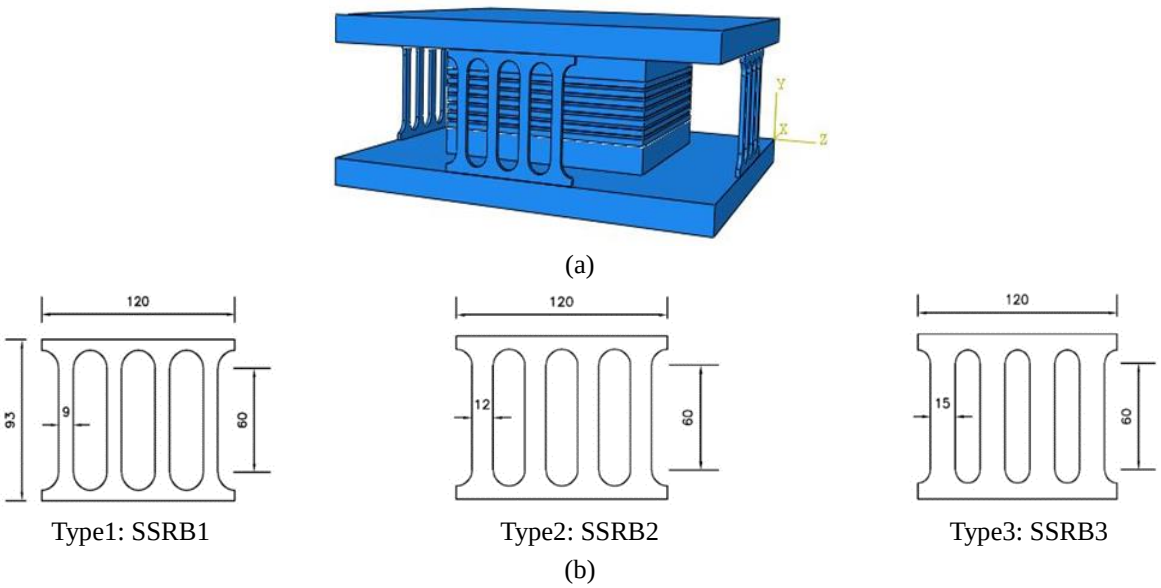

Fig. 6 (a) Full view of the SSRB. (b) Types of slit steel dampers (all dimensions are in mm)

isotropic material with modulus of elasticity of 210 MPa and Poisson's ratio of 0.3. For vertical stress of 7 MPa applied to the bearing 50% and 150% of the rubber shear strains and cyclic behavior of the isolator are yield and compared with the experimental results reported by (Abe *et al.* 2004), Fig. 5. This comparison confirms high accuracy of the presented analysis.

4. Description of FEM

Since slit steel rubber bearings are the subject of discussion in this study, the lead core of the LRB introduced in the previous section is removed and is replaced by slit steel dampers. The height of this slit damper is 92.8 mm equivalent to that of the vertical distance of the upper and lower steel plates of the bearing. As observed in Fig. 6(a), the slit dampers are arranged in a symmetrical manner on both sides of the bearing. In order to save time in analysis, the model scale is in half. In comparison to the original direction, the flexural strength of the slit damper in other directions is none of concern. So, the SSD in the bearing is examined in one direction. As shown in Fig. 6(b), three types of slit steel dampers are considered.

Slit steel dampers are modeled through the C3D8R element and mechanical behavior is assumed to be bilinear model with combined plastic. Also three different thicknesses are used for SSDs: 4, 6 and 8 mm. Two values are considered for yield stress of slit steel dampers as 240 MPa (st37 type) and 360 MPa (st52 type). Name of the bearings introduces their specifications (e.g., the SSRB1-st37-t4) is a type 1 SSRB with slits of 4 mm thickness made of st37.

5. Results and discussions

The hysteresis behavior of bearings such as horizontal stiffness, energy dissipation capacity, equivalent viscous damping and lateral forces transferred to the structure at each cycle are assessed here. These characteristics are defined in detail by (Saadatnia *et al.* 2019). In comparison with the lead core, slit dampers have high initial stiffness and do not experience large displacement. Dimensions of the slit dampers are assumed to be the same as those considered by (Chan and Albermani 2008), so the maximum displacement of these slit dampers are 17.5 mm, which is 50% of the shear strain of the laminated rubber. As to SSRB, the loading protocol for 10, 20, and 50% of the shear strain of the rubber corresponds to BSI BS EN 15129 (EN 2010).

Table 2 Operational characteristics of SSRB1 for different values of thicknesses and different steel type

	γ (%)	*SSRB1-t4-st37, **st52	*SSRB1-t6-st37, **st52	*SSRB1-t8-st37, **st52	LRB
Horizontal stiffness (kN/mm)	10	2.27, 2.91	3.17, 4.15	4.14, 5.54	2.26
	20	2.06, 2.47	2.71, 3.31	3.38, 4.22	1.69
	50	1.95, 2.61	2.88, 3.49	3.56, 4.42	1.23
	150	-	-	-	0.8
Dissipated energy (kJ)	10	0.07, 0.10	0.11, 0.15	0.15, 0.18	0.074
	20	0.22, 0.29	0.325, 0.42	0.44, 0.54	0.178
	50	0.89, 1.13	1.28, 1.60	1.66, 2.02	0.708
	150	-	-	-	2.4
Viscous damping (%)	10	41, 44	45, 47	47, 44	42
	20	34, 37	39, 41	41, 41	34
	50	27, 22	23, 23	24, 24	29
	150	-	-	-	17
Lateral force (kN)	10	6.80, 10.20	11, 14.5	14.45, 19.40	7.5
	20	14.1, 17.35	18.97, 23.22	23.66, 29.60	11.25
	50	36.95, 45.68	50.4, 61.17	62.3, 77.36	20
	150	-	-	-	43

* First value refers to slit damper made of st37 steel
** Second value refers to slit damper made of st52 steel

Table 3 Operational characteristics of SSRB2 for different values of thicknesses and different steel type

	γ (%)	*SSRB2-t4-st37, **st52	*SSRB2-t6-st37, **st52	*SSRB2-t8-st37, **st52	LRB
Horizontal stiffness (kN/mm)	10	3.92, 5.12	5.59, 7.24	7.41, 9.88	2.26
	20	3.10, 3.85	4.35, 5.21	5.48, 6.70	1.69
	50	2.75, 3.32	3.73, 4.38	4.70, 5.68	1.23
	150	-	-	-	0.8
Dissipated energy (kJ)	10	0.15, 0.18	0.20, 0.26	0.27, 0.36	0.074
	20	0.407, 0.50	0.58, 0.73	0.78, 0.97	0.178
	50	1.450, 1.83	2.05, 2.56	2.75, 3.44	0.708
	150	-	-	-	2.4
Viscous damping (%)	10	49, 46	46, 47	47, 47	42
	20	42, 43	43, 45	46, 45	34
	50	27, 28	28, 30	30, 31	29
	150	-	-	-	17
Lateral force (kN)	10	13.72, 17.93	19.60, 25.6	25.96, 34.60	7.5
	20	21.70, 26.97	30.46, 36.5	38.42, 48.78	11.25
	50	48.30, 58.25	65.37, 76	82.10, 99.48	20
	150	-	-	-	43

* First value refers to slit damper made of st37 steel
** Second value refers to slit damper made of st52 steel

Table 4 Operational characteristics of SSRB3 for different values of thicknesses and different steel type

	γ (%)	*SSRB3-t4-st37,**st52	*SSRB3-t6-st37,**st52	*SSRB3-t8-st37,**st52	LRB
Horizontal stiffness (kN/mm)	10	6.14, 8.08	8.93, 11.86	11.80, 15.75	2.26
	20	4.55, 5.74	6.46, 8.23	8.40, 10.75	1.69
	50	3.46, 4.20	4.78, 5.76	6.05, 7.30	1.23
	150	-	-	-	0.8
Dissipated energy (kJ)	10	0.22, 0.27	0.38, 0.43	0.43, 0.52	0.074
	20	0.64, 0.80	0.92, 1.17	1.16, 1.56	0.178
	50	2.15, 2.81	3.18, 4.06	4.18, 5.36	0.708
	150	-	-	-	2.4
Viscous damping (%)	10	46, 44	47, 47	47, 43	42
	20	46, 46	46, 46	45, 47	34
	50	32, 35	34, 36	36, 38	29
	150	-	-	-	17
Lateral force (kN)	10	21.50, 28.30	31.28, 41.50	41.32, 55.15	7.5
	20	31.84, 40.20	45.22, 57.60	58.76, 73.36	11.25
	50	60.65, 73.35	83.70, 100.90	105.83, 127.87	20
	150	-	-	-	43

* First value refers to slit damper made of st37 steel
** Second value refers to slit damper made of st52 steel

The characteristics of each isolator at every loading cycle are obtained by computing the SSRB behavior and comparing it with the LRB. In this comparison, first, the SSRB isolators are compared with different strip widths, SSD thicknesses and steel types at 10%, 20% and 50% shear strains, next, the main characteristics of the isolators are compared with that of the LRB characteristics as to 50% and 150% shear strains. For different types of isolator with various values of thickness presented in Table 2, values of the effective horizontal stiffness, energy dissipation capacity, equivalent viscous damping and the lateral force transferred to the structure are tabulated for SSRB1, SSRB2 and SSRB3 in Tables 2 to 4, respectively. For different values of thicknesses of SSRB1-st37, lateral force–deflection curves of the bearings are depicted in Fig. 7.

This figure shows that the yield strength of the isolator increases by increasing the thickness of SSD. This is consistent with Eqs. (1) and (2), which show a direct relation between the yield strength and SSD thickness. When the isolator experiences large displacements, the axial deformation of struts in tension occurs which increases stiffness and strength in this range of displacement (Maleki and Mahjoubi 2013).

As shown on the Tables 2, 3 and 4 for all three types of SSRBs by increasing the thickness of the plate, the effective stiffness of the isolator increases which can be explained by the direct relationship between the lateral stiffness of the SSD and its thickness. As the shear strain of the isolator increases, the effective horizontal stiffness decreases due to the plastic strain of the SSD. Fig. 7 shows that in the shear strain of 50%, the lowest effective horizontal stiffness of the isolators is related to the SSRB1-st37-4 which is about 123% higher than the horizontal stiffness of LRB in the same value of the shear strain. Increasing the SSD thickness leads to rise in the dissipated energy capacity. By

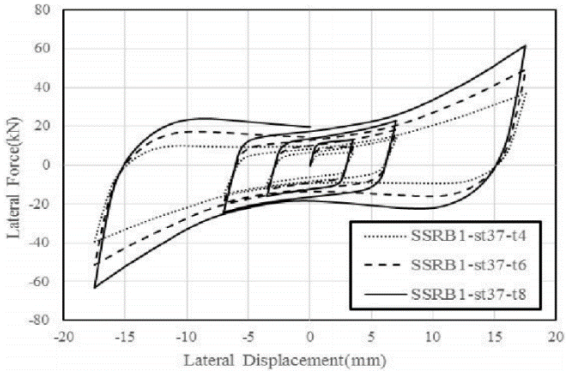

Fig. 7 Lateral force–deflection curve of SSRB1-st37 with different values of thickness

comparing the results of Tables 2, 3 and 4, the lowest energy dissipation is related to the SSRB1-st37-t4 isolator which is about 25% higher than the energy dissipation of the LRB at the same shear strain. SSD thickness has no significant effect on the equivalent viscous damping of the isolator. Actually, equivalent viscous damping has a direct and inverse relation with energy dissipation and effective stiffness, respectively. Increase in energy dissipation increases equivalent viscous damping while increase in effective stiffness decreases equivalent viscous damping.

On the other hand, increase in thickness increases both energy dissipation and effective stiffness of the isolator. Thus, at a specific value of the shear strain of the isolator, thickness has no considerable effect on viscous damping of the isolator.

It is observed that the lateral force transmitted to the superstructure increases with increase in value of SSD thickness. The lateral force of SSRB2-t8-st37 in the 20% shear strain, is near to the lateral force of LRB in 50% shear strain and the lateral force of the SSRB1-st52-t4 in the 50%

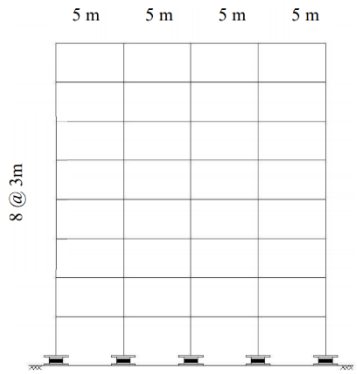

Fig. 8 Configuration of the frame used in this study

shear strain is approximately the same as that of the LRB in the 150% shear strain.

Changes in strut width on isolator behavior are similar to changes in SSD thickness. It can be seen that rise in the strut width leads to increase the effective stiffness, dissipated energy capacity, equivalent viscous damping and lateral force transmitted to the superstructure.

It was shown that values of effective horizontal stiffness, dissipated energy capacity, equivalent viscous damping and the transmitted lateral force to the structure for SSRB with SSD made of st52 are higher than corresponding values of SSRB with SSD made of st37. Numerical examples showed that value of the dissipated energy of SSRB-st52 is higher than the SSRB-st37 which is not noticeable in comparison with the effect of strut thickness and width.

SSRB is stiffer than LRB and also is more vulnerable to large deformation which is a drawback for this system. But the main advantage of SSRB is that it provides same amount of energy dissipation in comparison with LRB at a lower deformation and therefore seismic demand for displacement in SSRB is much less than seismic demand for displacement in LRB. Thus, it can be concluded that by selecting a suitable SSD, required lateral force can be achieved in much fewer displacements.

6. Effects of SSRB on structural performance

In this section, performance of structures equipped with SSRB is investigated. By presenting a case study, the advantages and disadvantages of SSRB in comparison with LRB are assessed. This case study is an 8-storey steel moment-resisting frame. Configuration of this frame is shown in Fig. 8. This frame is designed for 4 different cases: fixed-base, isolated with two different types of LRB and isolated with SSRB. ASCE7 (Merritt 1996) and AISC360 (ANSI 2010) codes are used to design the frame. It is assumed that the structure is located in a high seismicity region. The fundamental period of the fixed-base frame is about 1.4 seconds. Stiffness of LRBs for isolated structure is calculated based on the weight of the structure and the target period of the isolated structure. Two cases for isolated structure with LRB are considered: LRB-1 with fundamental period of 2.5 second and LRB-2 with

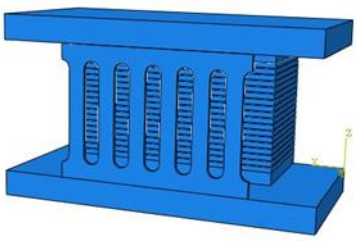

Fig. 9 Half of the SSRB used for 8-storey steel moment-resisting frame

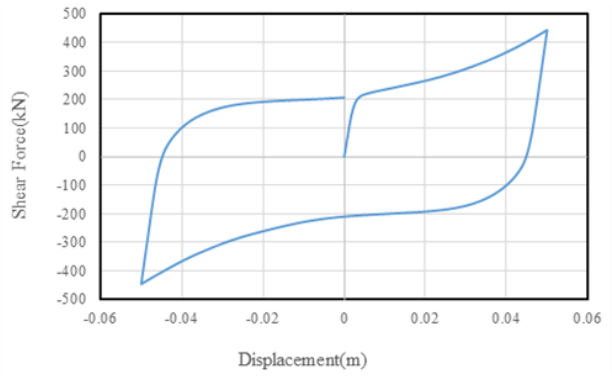

Fig. 10 Lateral force-deflection curve of SSRB

Table 5 Specifications of LRB-1, LRB-2 and SSRB

Isolator Type	$K_{eff}(\frac{kN}{m})$	$K_1(\frac{kN}{m})$	$F_y(kN)$	$\frac{K_1}{K_d}$	$D_D(m)$
LRB-1	656	4380	61	10	0.27
LRB-2	1265	17658	113	10	0.12
SSRB	9250	75000	180	14	0.05

fundamental period of 1.8 second.

LRB-1 is representative of an isolated structure with a soft isolator and its design is compatible with the main goal of seismic codes which try to elongate fundamental period of isolated structures. LRB-2 is representative of an isolated structure with a stiffer isolator. This case is selected because it is more similar to SSRB case and both these cases have isolators which are stiffer than the isolators designed based on seismic codes. Based on the stiffness of SSRB, the period shift in structures equipped with it is really small but fortunately SSRB can provide same amount of energy dissipation in comparison with LRB at a lower deformation. Therefore principles of designing base-isolated structures which is based on period shift cannot be used for structures equipped with SSRB. In other word, SSRB works as a combination of damper and bearing. Of course principle of designing a structure equipped with SSRB is out of scope of this paper but in summary it contains these steps: 1- Choosing the target displacement of isolator 2- Calculating the effective stiffness and damping 3- Calculating the energy dissipation and characteristic strength 4- Checking the isolator displacement. Designed SSRB is analyzed in ABAQUS software considering vertical load resulted from frame columns (Fig. 9).

The strut width in this SSRB is 50 mm and the thickness of its plate is 10 mm. Lateral force-deflection curve of the SSRB is shown in Fig. 10 up to 50 mm displacement, which

Table 6 Maximum displacement of isolators for seven records

Earthquake	SSRB	LRB-2	LRB-1
	d_{max} (mm)	d_{max} (mm)	d_{max} (mm)
Northridge	44	158	212
Duzce	25	126	348
Loma perieta	46	97	122
Erzincan	66	267	668
Imperial valley	20	93.5	219
Mendocino	22	96.5	147
Tabas	51	239	873
Average	39	153	369

is the acceptable displacement for this isolator. The specification of bilinear behavior of both the LRBs and SSRB are tabulated in Table 5. It should be mentioned that bilinear behavior is also used for the link element to model SSRB. Dynamic time history analyses are performed to compare the performance of fixed-base and three cases of isolated structures. Seven earthquake records which are scaled to the ASCE7 code response spectrum are used. Table 6 shows the maximum displacement of three isolators for seven records. As it can be seen, by increasing the flexibility of the isolator the demand displacement of isolator increases. The average displacement of the SSRB is 39 mm which is less that 50 mm. The base shears of the fixed-base frame and three cases of isolated frame are shown in Table 7.

Among the three isolators, the base shear reduction of LRB-1 due to the higher period of the building is larger than others. Although the stiffness of SSRB isolator is more than LRB-2 isolator, the base shear reduction of the SSRB and LRB-2 is approximately the same as compared to fixed-base structure. It can be judged that for SSRB with a lower capacity in displacement, proper performance can be achieved compared to LRB isolator with larger displacement capacity.

7. Conclusions

In this paper, using finite element analysis in ABAQUS software, performance of the slit steel rubber bearings was investigated. Isolators with different SSD thicknesses, strut width and steel type at different shear strains were studied. Performance of this isolator is compared with LRB performance. Finally, performance of an 8-storey frame equipped with SSRB and LRB has also been studied. Some important practical conclusions were provided through numerical results which can be declared as follows:

It was shown that increase in the thickness of slit steel plates leads to rise in value of the effective stiffness, dissipated energy capacity and lateral force transmitted to the superstructure, but thicknesses has no considerable effect on the equivalent viscous damping of the isolator. Numerical results showed that SSRB energy dissipation capacity can be larger than corresponding value of LRB. This capacity is obtained for SSRB at lower shear strain rather than LRB.

Table 7 Maximum base shear for fixed-base structure and three cases of isolated structures

Earthquake	Non-isolated structure	SSRB		LRB-1		LRB-2	
	F_{max} (kN)	F_{max} (kN)	Δ^*	F_{max} (kN)	Δ^*	F_{max} (kN)	Δ^*
Northridge	2856	2099	27%	740	74%	1931	32%
Duzce	2269	1544	32%	1039	54%	1638	28%
loma perieta	2760	2090	25%	542	80%	1378	50%
Erzincan	3053	2336	25%	1743	43%	2936	4%
Imperial valley	2341	1463	38%	755	67%	1348	42%
Mendocino	2519	1356	46%	598	76%	1374	45%
Tabas	3166	2256	29%	2193	30%	2673	15%
Average	2709	1877	32%	1087	61%	1897	31%

It was concluded that rise in the strut width leads to increase the effective stiffness, dissipated energy capacity, equivalent viscous damping and lateral force transmitted to the superstructure. The less the strut width the more the displacement capacity of the isolator. It was shown that values of effective horizontal stiffness, dissipated energy capacity, equivalent viscous damping and the transmitted lateral force to the structure for SSRB with SSD made of st52 are higher than corresponding values of SSRB with SSD made of st37.

By comparing a case study structure equipped with SSRB and LRB, it was shown that the base shear reduction as compared to fixed-base structure is more for structure equipped with LRB but if a stiffer LRB is used, results of SSRB and LRB in base shear reduction are compatible.

It was concluded that SSRB isolator is vulnerable to large deformation in comparison with conventional isolators like LRB. Based on the stiffness of SSRB, the period shift in small but fortunately SSRB can provide same amount of energy dissipation in comparison with LRB at a lower deformation. Therefore principles of designing base-isolated structures which is based on period shift cannot be used for structures equipped with SSRB. In other word, SSRB works as a combination of damper and bearing.

References

Abe, M., Yoshida, J. and Fujino, Y. (2004), "Multiaxial behaviors of laminated rubber bearings and their modeling. I: Experimental study", *J. Struct. Eng.*, **130**(8), 1119-1132. https://doi.org/10.1061/(ASCE)0733-9445(2004)130:8(1119).

Amadeo, B.C., Oh, S.H. and Akiyama, H. (1998), "Ultimate energy absorption capacity of slit-type steel plates subjected to shear deformations", *J. Struct. Constr. Eng.*, **63**(503), 139-147. https://doi.org/10.3130/aijs.63.139_1.

ANSI A (2010), AISC 360-10, Chicago, Illinois, U.S.A.

Asl, M.J., Rahman, M. and Karbakhsh, A. (2014), "Numerical analysis of seismic elastomeric isolation bearing in the base-isolated buildings", *Open J. Earthq. Res.* **3**(1), 1. https://doi.org/10.4236/ojer.2014.31001.

Bagheri, B., Choi, K.Y., Oh, S.H. and Ryu, H.S. (2016), "Shaking table test for evaluating the seismic response characteristics of concentrically braced steel structure with and without hysteretic

dampers", *Int. J. Steel Struct.*, **16**(1), 23-39. https://doi.org/10.1007/s13296-016-3003-2.

Bhuiyan, A.R., Okui, Y., Mitamura, H. and Imai, T. (2009), "A rheology model of high damping rubber bearings for seismic analysis: Identification of nonlinear viscosity", *Int. J. Solid. Struct.*, **46**(7-8), 1778-1792. https://doi.org/10.1016/j.ijsolstr.2009.01.005.

Chan, R.W. and Albermani, F. (2008), "Experimental study of steel slit damper for passive energy dissipation", *Eng. Struct.*, **30**(4), 1058-1066. https://doi.org/10.1016/j.engstruct.2007.07.005.

Choi, E., Nam, T.H. and Cho, B.S. (2005), "A new concept of isolation bearings for highway steel bridges using shape memory alloys", *Can. J. Civil Eng.*, **2**(5), 957-967. https://doi.org/10.1139/l05-049.

EN B (2010), 15129: 2009, Anti-Seismic Devices, BSI British Standards.

Ghobarah, A. and Ali, H. (1990), "Seismic design of base-isolated highway bridges utilizing lead-rubber bearings", *Can. J. Civil Eng.*, **17**(3), 413-422. https://doi.org/10.1139/l90-045.

Haeri, A., Badamchi, K. and Tajmir Riahi, H. (2019), "Proposing a new hybrid friction–yielding–elastomeric bearing", *J. Vib. Control*, **25**, 1558-1571. https://doi.org/10.1177/1077546319829535.

Hedayati Dezfuli, F. and Alam, M.S. (2017), "Smart lead rubber bearings equipped with ferrous shape memory alloy wires for seismically isolating highway bridges", *J. Earthq. Eng.*, **22**(6), 1042-1067. https://doi.org/10.1080/13632469.2016.1269692.

Iizuka, M. (2000), "A macroscopic model for predicting large-deformation behaviors of laminated rubber bearings", *Eng. Struct.*, **22**(4), 323-334. https://doi.org/ 10.1016/S0141-0296(98)00118-7.

Kalpakidis, I.V. and Constantinou, M.C. (2008), "Effects of heating and load history on the behavior of lead-rubber bearings", Technical Report MCEER-08-0027.

Kim, D., Oh, J., Do, J. and Park, J. (2014), "Effects of thermal aging on mechanical properties of laminated lead and natural rubber bearing", *Earthq. Struct.*, **6**(2), 127-140. https://doi.org/10.12989/eas.2014.6.2.127.

Kim, J. and Jeong, J. (2016), "Seismic retrofit of asymmetric structures using steel plate slit dampers", *J. Constr. Steel Res.*, **120**, 232-244. https://doi.org/10.1016/j.jcsr.2016.02.001.

Kim, J. and Shin, H. (2017), "Seismic loss assessment of a structure retrofitted with slit-friction hybrid dampers", *Eng. Struct.*, **130**, 336-350. https://doi.org/10.1016/j.engstruct.2016.10.052.

Lee, C.H., Kim, J., Kim, D.H., Ryu, J. and Ju, Y.K. (2016), "Numerical and experimental analysis of combined behavior of shear-type friction damper and non-uniform strip damper for multi-level seismic protection", *Eng. Struct.*, **114**, 75-92. https://doi.org/10.1016/j.engstruct.2016.02.007.

Lee, J. and Kim, J. (2015), "Seismic performance evaluation of moment frames with slit-friction hybrid dampers", *Earthq. Struct.*, **9**(6), 1291-1311. https://doi.org/10.12989/eas.2015.9.6.1291.

Lee, J., Kang, H. and Kim, J. (2017), "Seismic performance of steel plate slit-friction hybrid dampers", *J. Constr. Steel Res.*, **136**, 128-139. https://doi.org/10.1016/j.jcsr.2017.05.005.

Maleki, S. and Mahjoubi, S. (2013), "Dual-pipe damper", *J. Construct. Steel Res.*, **85**, 81-91. https://doi.org/10.1016/j.jcsr.2013.03.004.

Merritt, F. (1996), "Minimum design loads for buildings and other structures: American Society of Civil Engineers Standard 7-95", *J. Arch. Eng.*, **2**(2), 80-81.

Oh, S.H., Kim, Y.J. and Ryu, H.S. (2009), "Seismic performance of steel structures with slit dampers", *Eng. Struct.*, **31**(9), 1997-2008. https://doi.org/10.1016/j.engstruct.2013.08.011.

Paul, D. (2016), "Effect of lead in elastomeric bearings for structures located in seismic region", *Proc. Technol.*, **25**, 146-153. https://doi.org/10.1016/j.protcy.2016.08.091.

Ryan, K.L., Kelly, J.M. and Chopra, A.K. (2005), "Nonlinear model for lead-rubber bearings including axial-load effects", *J. Eng. Mech.*, **131**(12), 1270-1278. https://doi.org/10.1061/(ASCE)0733-9399(2005)131:12(1270).

Saadatnia, M., Riahi, H.T. and Izadinia, M. (2019), "Hysteretic behavior of rubber bearing with yielding shear devices", *Int. J. Steel Struct.*, **19**(3), 747-759. https://doi.org/10.1007/s13296-018-0159-y.

Saffari, H., Hedayat, A. and Nejad, M.P. (2013), "Post-Northridge connections with slit dampers to enhance strength and ductility", *J. Constr. Steel Res.*, **80**, 138-152. https://doi.org/10.1016/j.jcsr.2012.09.023.

Sanchez, J., Masroor, A., Mosqueda, G. and Ryan, K. (2012), "Static and dynamic stability of elastomeric bearings for seismic protection of structures", *J. Struct. Eng.*, **139**(7), 1149-1159. https://doi.org/10.1061/(ASCE)ST.1943-541X.0000660.

Sheikhi, J. and Fathi, M. (2019), "Natural rubber bearing incorporated with steel ring damper (NRB-SRD)", *Int. J. Steel Struct.*, 1-12. https://doi.org/10.1007/s13296-019-00267-7.

Tagawa, H., Yamanishi, T., Takaki, A. and Chan, R.W. (2016), "Cyclic behavior of seesaw energy dissipation system with steel slit dampers", *J. Constr. Steel Res.*, **117**, 24-34. https://doi.org/10.1016/j.jcsr.2015.09.014.

Talaeitaba, S.B., Pourmasoud, M.M. and Jabbari, M. (2019), "An innovative base isolator with steel rings and a rubber core", *Asian J. Civil Eng.*, **20**, 313-325. https://doi.org/10.1007/s42107-018-00107-9.

Tiong, P.L., Adnan, A., Rahman, A. and Mirasa, A.K. (2014), "Seismic base isolation of precast wall system using high damping rubber bearing", *Earthq. Struct.*, **7**(6), 1141-1169. https://doi.org/10.12989/eas.2014.7.6.1141.

Yoon, H., Kwahk, I.J. and Kim, Y.J. (2013), "A study on the ultimate performances of elastomeric bearings in Korea", *KSCE J. Civil Eng.*, **17**(2), 438-449. https://doi.org/.10.1007/s12205-013-1398-2.

Zhou, T., Wu, Y.F. and Li, A.Q. (2018), "Numerical study on the ultimate behavior of elastomeric bearings under combined compression and shear", *KSCE J. Civil Eng.*, **22(**9), 3556-3566. https://doi.org/10.1007/s12205-018-0949-y.

CC